Acta Cryst E CRYSTALLOGRAPHIC COMMUNICATIONS

ISSN 2056-9890

Syntheses and crystal structures of the quaternary thiogermanates $Cu_4FeGe_2S_7$ and $Cu_4CoGe_2S_7$

Andrew J. Craig, Stanislav S. Stoyko, Allyson Bonnoni and Jennifer A. Aitken*

Department of Chemistry and Biochemistry, Duquesne University, 600 Forbes Ave, Pittsburgh PA 15282, USA. *Correspondence e-mail: aitkenj@duq.edu

Received 27 May 2020
Accepted 10 June 2020

Edited by W. T. A. Harrison, University of Aberdeen, Scotland

Keywords: crystal structure; diamond-like; thiogermanate; quaternary sulfide.

CCDC references: 2009145; 2009144

Supporting information: this article has supporting information at journals.iucr.org/e

The quaternary thiogermanates $Cu_4FeGe_2S_7$ (tetracopper iron digermanium heptasulfide) and $Cu_4CoGe_2S_7$ (tetracopper cobalt digermanium heptasulfide) were prepared in evacuated fused-silica ampoules *via* high-temperature, solid-state synthesis using stoichiometric amounts of the elements at 1273 K. These isostructural compounds crystallize in the $Cu_4NiSi_2S_7$ structure type, which can be considered as a superstructure of cubic diamond or sphalerite. The monovalent (Cu^+), divalent (Fe^{2+} or Co^{2+}) and tetravalent (Ge^{4+}) cations adopt tetrahedral geometries, each being surrounded by four S^{2-} anions. The divalent cation and one of the sulfide ions lie on crystallographic twofold axes. These tetrahedra share corners to create a three-dimensional framework structure. All of the tetrahedra align along the same crystallographic direction, rendering the structure non-centrosymmetric and polar (space group *C*2). Analysis of X-ray powder diffraction data revealed that the structures are the major phase of the reaction products. Thermal analysis indicated relatively high melting temperatures, near 1273 K.

1. Chemical context

The title compounds belong to the family of quaternary thiogermanates, which can be constructed from different $[Ge_xS_y]^{z-}$ building blocks, such as $[GeS_4]^{4-}$ (Aitken *et al.*, 2001) and $[Ge_2S_6]^{4-}$ (Choudhury *et al.*, 2015). Two GeS_4 tetrahedra can share a corner to create $[Ge_2S_7]^{6-}$ units, which are featured in the title compounds. $Cu_4FeGe_2S_7$ and $Cu_4CoGe_2S_7$ also belong to the family of diamond-like semiconductors (DLSs), with structures that can be derived from the cubic or hexagonal (Frondel & Marvin, 1967) forms of diamond. The synthesis of new diamond-like materials is guided by valence electron principles and Pauling's rules, and the resulting DLSs can be binary, ternary, or quaternary, depending on the number of elements employed in the reaction (Parthé, 1964; Pamplin, 1981; Goryunova, 1965). Increasing the number of elements in the formula allows for greater tunability of the material's properties; thus, quaternary DLSs are a particularly appealing class of materials. As a result of their technologically relevant properties, these materials are of interest for a number of applications, such as solar cells (Ito & Nakazawa, 1988; Heppke *et al.*, 2020; Liu *et al.*, 2018), batteries (Brant, Devlin *et al.*, 2015; Kaib *et al.*, 2013) and magnetic devices (Wintenberger, 1979; Greenwood & Whitfield, 1968). Furthermore, owing to their inherently non-centrosymmetric structures, DLSs are attractive candidates for infrared non-linear optical (IR–NLO) devices that make use of second-harmonic generation (SHG) crystals (Ohmer & Pandey 1998): only crystals that lack an inversion center can exhibit SHG.

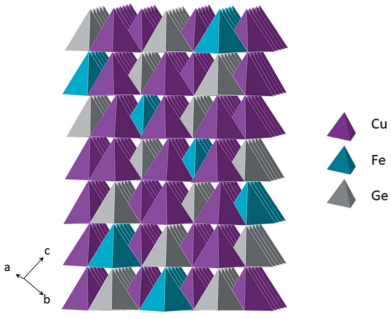

IR–NLO materials are used to shift the radiation of lasers to more suitable wavelengths for use in military (Hopkins 1998), medical (Stoeppler *et al.*, 2012) and industrial applications (Bamford *et al.*, 2007). Currently, ternary DLSs, most of which are sulfides, dominate the market of SHG crystals for use in the infrared (Ohmer & Pandey, 1998). Yet the current commercially available IR–NLO materials suffer from serious drawbacks, such as low laser-induced damage thresholds (LIDTs) and multi-photon absorption (Schunemann, 2007). Turning attention to the discovery of new quaternary DLSs provides a reliable route to next-generation IR–NLO materials that allows for greater control of the material's properties. Compounds such as Li_2CdGeS_4 (Brant, Clark *et al.*, 2014), Li_2MnGeS_4 (Brant, Clark *et al.*, 2015), and $Li_4HgGe_2S_7$ (Wu, Yang & Pan, 2017) have shown potential to outperform currently used ternary IR–NLO crystals. These DLSs have shown promising SHG capabilities, as well as resilience to high powered lasers, a necessity to broaden future usage (Hopkins, 1998). For these reasons, we were motivated to investigate the Cu–Fe–Ge–S and Cu–Co–Ge–S systems for new DLSs.

2. Structural commentary

The title compounds, $Cu_4FeGe_2S_7$ (I) and $Cu_4CoGe_2S_7$ (II), are isostructural and crystallize in the non-centrosymmetric, monoclinic space group *C*2 (No. 5) with the $Cu_4NiSi_2S_7$ structure type (Schäfer *et al.*, 1980). The structure contains two crystallographically unique Cu^+ ions, one divalent metal (Fe or Co) sited on a crystallographic twofold axis, one Ge^{4+} cation and four S^{2-} anions (one with site symmetry 2) (Fig. 1). The sulfide anions create a 'cubic' close-packed array and the cations reside in one-half of the tetrahedral holes; these tetrahedra share corners to form a three-dimensional network. Two GeS_4 tetrahedra share corners to form $(Ge_2S_7)^{6-}$ subunits that are isolated from each other (Fig. 1). These subunits are separated by isolated FeS_4 tetrahedra and surrounded by a snaking, three-dimensional network of corner-sharing CuS_4 tetrahedra that serve to link the $(Ge_2S_7)^{6-}$ and FeS_4 subunits. All of the tetrahedra are aligned along one crystallographic direction, rendering the structure non-centrosymmetric (Fig. 2). All DLSs exhibit a honeycomb pattern in their crystal structure (Fig. 3); the various resulting space groups arise from the different possible cation-ordering patterns.

Selected geometrical data for (I) and (II) are given in Tables 1 and 2, respectively. The average Fe—S (I) and Co—S (II) bond distances are 2.334 (6) and 2.317 (6) Å, respectively. These values align well with other compounds containing iron or cobalt tetrahedrally coordinated by sulfur. For example, the average Fe—S distance found in Li_2FeGeS_4 is 2.34 (2) Å

Table 1
Selected bond lengths (Å) for (I).

Cu1—S3^{i}	2.290 (2)	Fe—S4^{v}	2.331 (3)
Cu1—S3	2.302 (2)	Fe—S4	2.331 (3)
Cu1—S2^{ii}	2.303 (2)	Fe—S2^{iv}	2.337 (3)
Cu1—S1^{iii}	2.353 (2)	Fe—S2^{vi}	2.337 (3)
Cu2—S3	2.294 (2)	Ge—S3^{vii}	2.196 (2)
Cu2—S2	2.309 (2)	Ge—S2	2.221 (2)
Cu2—S4^{iv}	2.309 (2)	Ge—S4^{iii}	2.233 (2)
Cu2—S4	2.319 (2)	Ge—S1^{iii}	2.3107 (19)

Symmetry codes: (i) $-x+\frac{3}{2}, y-\frac{1}{2}, -z+2$; (ii) $x, y-1, z$; (iii) $x-\frac{1}{2}, y-\frac{1}{2}, z$; (iv) $-x+\frac{3}{2}, y-\frac{1}{2}, -z+1$; (v) $-x+2, y, -z+1$; (vi) $x+\frac{1}{2}, y-\frac{1}{2}, z$; (vii) $x-\frac{1}{2}, y+\frac{1}{2}, z$.

Table 2
Selected bond lengths (Å) for (II).

Cu1—S3^{i}	2.292 (2)	Co—S4^{v}	2.308 (3)
Cu1—S2^{ii}	2.295 (2)	Co—S4	2.308 (3)
Cu1—S3	2.304 (2)	Co—S2^{iv}	2.325 (3)
Cu1—S1^{iii}	2.343 (3)	Co—S2^{vi}	2.325 (3)
Cu2—S3	2.290 (2)	Ge—S2	2.211 (3)
Cu2—S2	2.298 (3)	Ge—S3^{vii}	2.211 (2)
Cu2—S4^{iv}	2.301 (2)	Ge—S4^{iii}	2.236 (2)
Cu2—S4	2.311 (2)	Ge—S1^{iii}	2.316 (2)

Symmetry codes: (i) $-x+\frac{3}{2}, y-\frac{1}{2}, -z+2$; (ii) $x, y-1, z$; (iii) $x-\frac{1}{2}, y-\frac{1}{2}, z$; (iv) $-x+\frac{3}{2}, y-\frac{1}{2}, -z+1$; (v) $-x+2, y, -z+1$; (vi) $x+\frac{1}{2}, y-\frac{1}{2}, z$; (vii) $x-\frac{1}{2}, y+\frac{1}{2}, z$.

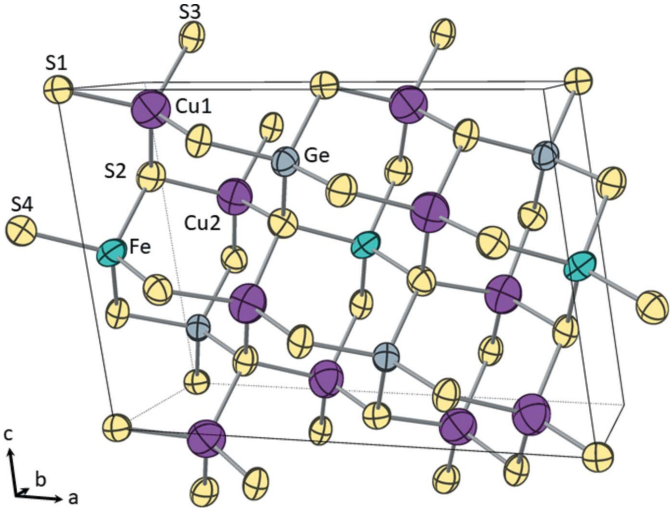

Figure 1
The structure of $Cu_4FeGe_2S_7$ with crystallographically unique ions labeled. Ellipsoids are shown at 99% probability. $Cu_4CoGe_2S_7$ is isostructural and has similar atomic displacement parameters.

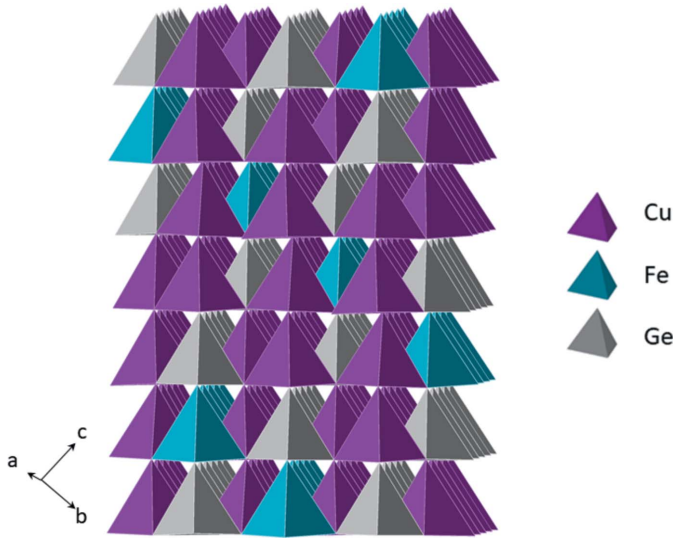

Figure 2
Polyhedral view of $Cu_4FeGe_2S_7$ showing the polar nature of the structure.

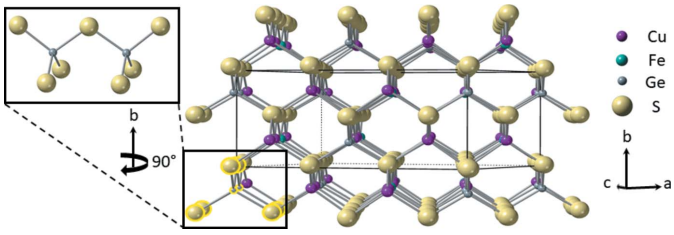

Figure 3
The 'honeycomb' pattern found in $Cu_4FeGe_2S_7$, a characteristic of DLSs. Highlighted in the bottom left corner is one of the $[Ge_2S_7]^{6-}$ subunits that forms in this structure.

(Brant, dela Cruz *et al.*, 2014), while the average Co—S distance found in Li_2CoGeS_4 is 2.31 (3) Å (Brant, Devlin *et al.*, 2015). The average Ge—S distances are 2.240 (4) and 2.244 (5) Å for (I) and (II), respectively. These distances are also close to those of the lithium-containing DLSs: Li_2FeGeS_4 (Brant, Devlin *et al.*, 2015) and Li_2CoGeS_4 (Brant, dela Cruz *et al.*, 2014) possess values of 2.23 (2) and 2.22 (3) Å, respectively. The average tetrahedral bond angles for all cations in both title compounds is, within uncertainty, ideal. For comparison, the tetrahedral angular ranges encountered in Cu_2FeGeS_4 (Wintenberger, 1979) and Cu_2CoGeS_4 (Gulay *et al.*, 2004) are 109.471–109.484° and 109.473–109.579°, respectively. The sulfur anions also exhibit tetrahedral coordination. Both S2 and S4 are coordinated by two copper, one germanium and one iron or cobalt cation. S1 is connected to two germanium and two copper cations, while S3 is surrounded by one germanium and three copper cations.

3. Database survey

Quaternary DLSs exist with several different formulae; examples that incorporate chalcogenides as the anion are $I–II_2–III–VI_4$, $I_2–II–IV–VI_4$, and $I_4–II–IV_2–VI_7$. In these formulae, the Roman numerals represent the number of valence electrons for each element. Compounds of the formula $I–II_2–III–VI_4$, such as $CuMn_2InS_4$ (Delgado & Sagredo, 2016) and $CuFe_2InSe_4$ (Delgado *et al.*, 2008) include trivalent elements, while the other relevant formulae mentioned above, including the title compounds, contain tetravalent elements. Numerous DLSs of the general formula $I_2–II–IV–VI_4$ have been reported and crystallize in non-centrosymmetric space groups, such as $I\bar{4}2m$ and $Pmn2_1$ with the stannite and wurtz-stannite structure types that are derived from the cubic and hexagonal diamond structures, respectively (Brunetta *et al.*, 2013). The monovalent ions incorporated in these materials include Li (Wu, Zhang, *et al.*, 2017; Wu & Pan, 2017), Cu (Parthé *et al.*, 1969) or Ag (Brunetta *et al.*, 2013) and the divalent ions include a number of metals, such as Mg (Liu *et al.*, 2013), Mn (Bernert & Pfitzner, 2005), Fe (Wintenberger, 1979), Co (Bernert and Pfitzner 2006), Zn (Parasyuk *et al.*, 2001), Cd (Rosmus *et al.*, 2014) and Hg (Olekseyuk *et al.*, 2005). The tetravalent ions found in these compounds are usually Si, Ge, or Sn, while the hexavalent atoms (*i.e.*, the divalent anions) can be S (Lekse *et al.*, 2009), Se (Gulay, Romanyuk & Parasyuk, 2002), or Te (Parasyuk *et al.*, 2005). Some specific examples include Cu_2MgGeS_4 (Liu *et al.*, 2013) and Ag_2MnSnS_4 (Friedrich *et al.*, 2018).

In contrast, considerably fewer compounds of the general formula $I_4–II–IV_2–VI_7$ have been discovered: only seven of these, which crystallize in either space group *C*2 or *Cc* with structures derived from cubic or hexagonal diamond, respectively, have been published to date: $Li_4MnGe_2S_7$ (*Cc*) (Kaib *et al.*, 2013), $Li_4MnSn_2Se_7$ (*Cc*) (Kaib *et al.*, 2013), $Li_4HgGe_2S_7$ (*Cc*) (Wu, Yang, Pan 2017), $Ag_4HgGe_2S_7$ (*Cc*) (Gulay, Olekseyuk & Parasyuk 2002), $Ag_4CdGe_2S_7$ (*Cc*) (Gulay, Olekseyuk & Parasyuk 2002), $Cu_4NiSi_2S_7$ (*C*2) (Schäfer *et al.*, 1980), and $Cu_4NiGe_2S_7$ (*C*2) (Schäfer *et al.*, 1980).

4. X-ray powder diffraction and thermal analysis

The calculated and observed X-ray powder diffraction patterns match well (Fig. 4), indicating that the title compounds are the major phases of the respective reactions. An optimization of the synthetic protocol is needed to isolate the desired phases in phase-pure form.

Differential thermal analysis (DTA) reveals that $Cu_4FeGe_2S_7$ and $Cu_4CoGe_2S_7$ show relatively high thermal stability and melting and recrystallization events with appropriate hysteresis around 1000°C (Fig. 5). Multiple heating-cooling cycles for each sample were consistent, suggesting that the thermal events are reversible. X-ray powder diffraction of the DTA residues indicated that the samples were not changed by the thermal analyses, implying that they melt congruently. DTA also suggests that neither compound is a single phase, as

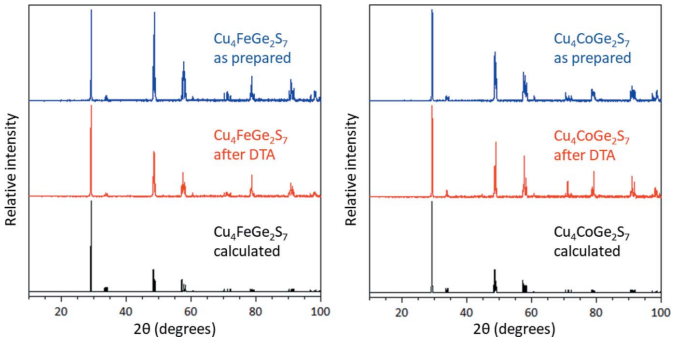

Figure 4
Comparison of experimental X-ray powder diffraction patterns before and after DTA with those calculated using the single-crystal structures for $Cu_4FeGe_2S_7$ (left) and $Cu_4CoGe_2S_7$ (right).

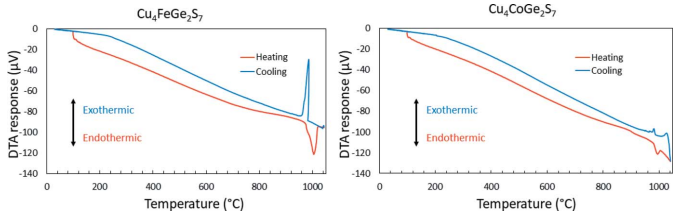

Figure 5
Differential thermal analysis diagrams obtained for the title compounds showing the melting and recrystallization events.

Table 3
Experimental details.

	(I)	(II)
Crystal data		
Chemical formula	$Cu_4FeGe_2S_7$	$Cu_4CoGe_2S_7$
M_r	679.61	682.69
Crystal system, space group	Monoclinic, *C*2	Monoclinic, *C*2
Temperature (K)	296	296
a, *b*, *c* (Å)	11.7405 (6), 5.3589 (2), 8.3420 (4)	11.7280 (2), 5.33987 (10), 8.33133 (14)
β (°)	98.661 (3)	98.6680 (12)
V (Å^3)	518.86 (4)	515.80 (2)
Z	2	2
Radiation type	Mo *K*α	Mo *K*α
μ (mm^{-1})	16.46	16.76
Crystal size (mm)	0.08 × 0.08 × 0.03	0.08 × 0.07 × 0.06
Data collection		
Diffractometer	Bruker SMART APEXII	Bruker SMART APEXII
Absorption correction	Multi-scan (*SADABS*; Sheldrick, 2002)	Multi-scan (*SADABS*; Sheldrick, 2002)
T_{min}, T_{max}	0.246, 0.435	0.356, 0.435
No. of measured, independent and observed [$I > 2\sigma(I)$] reflections	2258, 1187, 994	2239, 1177, 1039
R_{int}	0.021	0.017
(sin $\theta/\lambda)_{max}$ (Å^{-1})	0.649	0.649
Refinement		
$R[F^2 > 2\sigma(F^2)]$, $wR(F^2)$, *S*	0.034, 0.094, 1.06	0.030, 0.075, 1.11
No. of reflections	1187	1177
No. of parameters	67	67
No. of restraints	1	1
$\Delta\rho_{max}$, $\Delta\rho_{min}$ (e Å^{-3})	0.75, −0.89	0.88, −0.49
Absolute structure	Flack (1983)	Flack (1983)
Absolute structure parameter	0.06 (3)	0.06 (3)

Computer programs: *SMART* and *SAINT* (Bruker, 1998), *SHELXS97* (Sheldrick, 2008), *SHELXL2018/3* (Sheldrick, 2015) and *CrystalMaker* (Palmer, 2014).

there are some small shoulders on the peaks indicative of the thermal events.

5. Materials and methods

All powdered elements were acquired from commercial suppliers and used as obtained with the exception of germanium metal, which was purchased as chunks and ground to a fine powder using a Diamonite™ mortar and pestle prior to use. Powder X-ray diffraction data were recorded from 10–100° 2θ using a PANalytical X'Pert Pro MPD powder X-ray diffractometer operating with Cu K_α radiation (λ = 1.541871 Å), a tube power of 45 kV and 40 mA and a step size of 0.017°. DTA data were obtained using a Shimadzu DTA50 thermal analyzer. Each sample was vacuum-sealed in a fused-silica ampoule, placed alongside an ampoule containing an Al_2O_3 reference of comparable mass, heated from room temperature to 1050°C at a rate of 10°C min^{-1} and subsequently cooled to room temperature at the same rate. A second heating–cooling cycle was conducted in order to determine the reproducibility of the thermal events.

6. Synthesis and crystallization

$Cu_4FeGe_2S_7$ and $Cu_4CoGe_2S_7$ were synthesized by combining stoichiometric amounts of Cu (99.999%), Fe (99.99%) or Co (99.99%), Ge (99.999%) and S (99.5%, sublimed) powders. The powders were mixed and placed into 12 mm o.d. fused-silica tubes that were subsequently attached to a vacuum line, evacuated and flame sealed. The reaction vessels were placed upright into ceramic containers inside programmable furnaces, where they were heated to 1000°C in 24 h, held there for 48 h, cooled to 900°C over the course of 50 h, and held there for 96 h, before being allowed to cool to room temperature over a 24 h period. Subsequently, the reaction vessels were cut open and the contents were examined under a light microscope. The products consisted of loose silvery gray microcrystalline powders from which small single crystals were selected for single-crystal X-ray diffraction.

7. Refinement

Crystal data, data collection parameters, and structure refinement details are summarized in Table 3. Extinction parameters were refined for each compound. After the final refinement, the Flack parameter for both structures refined to 0.06 (3), indicating that the absolute structure is correct. In $Cu_4FeGe_2S_7$, the largest difference peak is located 1.15 Å from Cu2 while the deepest difference hole is 1.50 Å from S3. For $Cu_4CoGe_2S_7$, the largest difference peak is 0.67 Å from Co while the deepest difference hole is 0.83 Å from Ge.

Acknowledgements

We gratefully acknowledge Mr Daniel J. Bodnar, instrument maintenance manager of the Bayer School of Natural and

Environmental Sciences at Duquesne University, for keeping the diffractometers running.

Funding information

This research was supported by the National Science Foundation, Division of Materials Research under grant No. DMR-1611198. The single-crystal and powder X-ray diffractometers were purchased with funds from the National Science Foundation under grant Nos. CHE-0234872 and DUE-0511444, respectively.

References

Aitken, J. A., Larson, P., Mahanti, S. D. & Kanatzidis, M. G. (2001). *Chem. Mater.* **13**, 4714–4721.
Bamford, D. J., Cook, D. J., Sharpe, S. J. & Van Pelt, A. D. (2007). *Appl. Opt.* **46**, 3958–3968.
Bernert, T. & Pfitzner, A. (2005). *Z. Kristallogr.* **220**, 968–972.
Bernert, T. & Pfitzner, A. (2006). *Z. Anorg. Allg. Chem.* **632**, 1213–1218.
Brant, J. A., Clark, D. J., Kim, Y. S., Jang, J. I., Weiland, A. & Aitken, J. A. (2015). *Inorg. Chem.* **54**, 2809–2819.
Brant, J. A., Clark, D. J., Kim, Y. S., Jang, J. I., Zhang, J.-H. & Aitken, J. A. (2014). *Chem. Mater.* **26**, 3045–3048.
Brant, J. A., dela Cruz, C., Yao, J., Douvalis, A. P., Bakas, T., Sorescu, M. & Aitken, J. A. (2014). *Inorg. Chem.* **53**, 12265–12274.
Brant, J. A., Devlin, K. P., Bischoff, C., Watson, D., Martin, S. W., Gross, M. D. & Aitken, J. A. (2015). *Solid State Ionics*, **278**, 268–274.
Bruker (1998). *SMART* and *SAINT*. Bruker AXS Inc., Madison, Wisconsin, USA.
Brunetta, C. D., Brant, J. A., Rosmus, K. A., Henline, K. M., Karey, E., MacNeil, J. H. & Aitken, J. A. (2013). *J. Alloys Compd.* **574**, 495–503.
Choudhury, A., Ghosh, K., Grandjean, F., Long, G. J. & Dorhout, P. K. (2015). *J. Solid State Chem.* **226**, 74–80.
Delgado, G. E., Mora, A. J., Grima-Gallardo, P. & Quintero, M. (2008). *J. Alloys Compd.* **454**, 306–309.
Delgado, G. E. & Sagredo, V. (2016). *Bull. Mater. Sci.* **39**, 1631–1634.
Flack, H. D. (1983). *Acta Cryst.* A**39**, 876–881.
Friedrich, D., Greil, S., Block, T., Heletta, L., Pöttgen, R. & Pfitzner, A. (2018). *Z. Anorg. Allg. Chem.* **644**, 1707–1714.
Frondel, C. & Marvin, U. B. (1967). *Nature*, **214**, 587–589.
Goryunova, N. A. (1965). T*he Chemistry of Diamond-like Semiconductors*. Cambridge, MA: Massachusetts Institute of Technology.
Greenwood, N. N. & Whitfield, H. J. (1968). *J. Chem. Soc. A*, pp. 1697–1699.
Gulay, L. D., Nazarchuk, O. P. & Olekseyuk, I. D. (2004). *J. Alloys Compd.* **377**, 306–311.
Gulay, L. D., Olekseyuk, I. D. & Parasyuk, O. V. (2002). *J. Alloys Compd.* **340**, 157–166.
Gulay, L. D., Romanyuk, Y. E. & Parasyuk, O. V. (2002). *J. Alloys Compd.* **347**, 193–197.
Heppke, E. M., Berendts, S. & Lerch, M. (2020). *Z. Naturforsch. Teil B*, **75**, 393–402.
Hopkins, F. K. (1998). *Opt. Photonics News*, **9**, 32-38.
Ito, K. & Nakazawa, T. (1988). *Jpn. J. Appl. Phys.* **27**, 2094–2097.
Kaib, T., Haddadpour, S., Andersen, H. F., Mayrhofer, L., Järvi, T. T., Moseler, M., Möller, K.-C. & Dehnen, S. (2013). *Adv. Funct. Mater.* **23**, 5693–5699.
Lekse, J. W., Moreau, M. A., McNerny, K. L., Yeon, J., Halasyamani, P. S. & Aitken, J. A. (2009). *Inorg. Chem.* **48**, 7516–7518.
Liu, B.-W., Zhang, M.-J., Zhao, Z., Zeng, H.-Y., Zheng, F.-K., Guo, G.-C. & Huang, J.-S. (2013). *J. Solid State Chem.* **204**, 251–256.
Liu, Q., Cai, Z., Han, D. & Chen, S. (2018). *Sci. Rep.* **8**, 1604.
Ohmer, M. C. & Pandey, R. (1998). *MRS Bull.* **23**, 16–22.
Olekseyuk, I. D., Marchuk, O. V., Gulay, L. D. & Zhbankov, O. Y. (2005). *J. Alloys Compd.* **398**, 80–84.
Palmer, D. C. (2014). *CrystalMaker*. CrystalMaker Software Ltd, Begbroke, Oxfordshire, England.
Pamplin, B. (1981). *Prog. Crystl. Growth Charact.* **3**, 179–192.
Parasyuk, O. V., Gulay, L. D., Romanyuk, Y. E. & Piskach, L. V. (2001). *J. Alloys Compd.* **329**, 202–207.
Parasyuk, O. V., Olekseyuk, I. D. & Piskach, L. V. (2005). *J. Alloys Compd.* **397**, 169–172.
Parthé, E., Yvon, K. & Deitch, R. H. (1969). *Acta Cryst.* B**25**, 1164–1174.
Parthé, E. (1964). *Crystal Chemistry of Tetrahedral Structures*. New York: Gordon and Breach Science Publishers.
Rosmus, K. A., Brant, J. A., Wisneski, S. D., Clark, D. J., Kim, Y. S., Jang, J. I., Brunetta, C. D., Zhang, J.-H., Srnec, M. N. & Aitken, J. A. (2014). *Inorg. Chem.* **53**, 7809–7811.
Schäfer, W., Scheunemann, K. & Nitsche, R. (1980). *Mater. Res. Bull.* **15**, 933–937.
Schunemann, P. G. (2007). *Proc. SPIE*, **6455**, 64550R.
Sheldrick, G. M. (2002). *SADABS*. University of Göttingen, Germany.
Sheldrick, G. M. (2008). *Acta Cryst*. A**64**, 112–122.
Sheldrick, G. M. (2015). *Acta Cryst.* C**71**, 3–8.
Stoeppler, G., Schellhorn, M. & Eichhorn, M. (2012). *Laser Phys.* **22**, 1095–1098.
Wintenberger, M. (1979). *Mater. Res. Bull.* **14**, 1195–1202.
Wu, K. & Pan, S. (2017). *Crystals*, **7**, 107.
Wu, K., Yang, Z. & Pan, S. (2017). *Chem. Commun.* **53**, 3010–3013.
Wu, K., Zhang, B., Yang, Z. & Pan, S. (2017). *J. Am. Chem. Soc.* **139**, 14885–14888.

supporting information

Acta Cryst. (2020). E**76**, 1117-1121 [https://doi.org/10.1107/S2056989020007872]

Syntheses and crystal structures of the quaternary thiogermanates $Cu_4FeGe_2S_7$ and $Cu_4CoGe_2S_7$

Andrew J. Craig, Stanislav S. Stoyko, Allyson Bonnoni and Jennifer A. Aitken

Computing details

For both structures, data collection: *SMART* (Bruker, 1998); cell refinement: *SAINT* (Bruker, 1998); data reduction: *SAINT* (Bruker, 1998); program(s) used to solve structure: *SHELXS97* (Sheldrick, 2008); program(s) used to refine structure: *SHELXL2018/3* (Sheldrick, 2015); molecular graphics: *CrystalMaker* (Palmer, 2014); software used to prepare material for publication: *SHELXL2018/3* (Sheldrick, 2015).

Tetracopper iron digermanium heptasulfide (I)

Crystal data

$Cu_4FeGe_2S_7$
M_r = 679.61
Monoclinic, *C*2
a = 11.7405 (6) Å
b = 5.3589 (2) Å
c = 8.3420 (4) Å
β = 98.661 (3)°
V = 518.86 (4) Å^3
Z = 2
F(000) = 636
D_x = 4.350 Mg m^{-3}
Mo *Kα* radiation, *λ* = 0.71073 Å
Cell parameters from 4891 reflections
θ = 4.2–31.4°
μ = 16.46 mm^{-1}
T = 296 K
Irregular, grey
0.08 × 0.08 × 0.03 mm

Data collection

Bruker SMART APEXII diffractometer
φ and *ω* Scans scans
Absorption correction: multi-scan (SADABS; Sheldrick, 2002)
T_{min} = 0.246, T_{max} = 0.435
2258 measured reflections
1187 independent reflections
994 reflections with $I > 2\sigma(I)$
R_{int} = 0.021
θ_{max} = 27.5°, θ_{min} = 2.5°
h = −15→15
k = −6→6
l = −10→10

Refinement

Refinement on F^2
Least-squares matrix: full
$R[F^2 > 2\sigma(F^2)]$ = 0.034
$wR(F^2)$ = 0.094
S = 1.06
1187 reflections
67 parameters
1 restraint
Primary atom site location: structure-invariant direct methods
$w = 1/[\sigma^2(F_o^2) + (0.0315P)^2]$ where $P = (F_o^2 + 2F_c^2)/3$
$(\Delta/\sigma)_{max} < 0.001$
$\Delta\rho_{max}$ = 0.75 e Å^{-3}
$\Delta\rho_{min}$ = −0.89 e Å^{-3}
Extinction correction: SHELXL-2018/3 (Sheldrick 2018), $Fc^*=kFc[1+0.001xFc^2\lambda^3/\sin(2\theta)]^{-1/4}$
Extinction coefficient: 0.0123 (9)
Absolute structure: Flack (1983)
Absolute structure parameter: 0.06 (3)

Special details

Geometry. All esds (except the esd in the dihedral angle between two l.s. planes) are estimated using the full covariance matrix. The cell esds are taken into account individually in the estimation of esds in distances, angles and torsion angles; correlations between esds in cell parameters are only used when they are defined by crystal symmetry. An approximate (isotropic) treatment of cell esds is used for estimating esds involving l.s. planes.

Refinement. Refined as a two-component inversion twin

Fractional atomic coordinates and isotropic or equivalent isotropic displacement parameters (Å²)

	x	*y*	*z*	U_{iso}*/U_{eq}
Cu1	0.64298 (8)	0.2054 (3)	0.93484 (11)	0.0174 (7)
Cu2	0.71147 (8)	0.7098 (2)	0.64229 (10)	0.0165 (6)
Fe	1.000000	0.7200 (6)	0.500000	0.0112 (6)
Ge	0.42524 (6)	0.7285 (3)	0.78371 (7)	0.0092 (3)
S1	1.000000	0.9789 (6)	1.000000	0.0091 (6)
S2	0.56834 (15)	0.9593 (5)	0.71791 (18)	0.0111 (6)
S3	0.78390 (14)	0.4527 (4)	0.85310 (17)	0.0091 (6)
S4	0.85688 (15)	0.9704 (5)	0.58180 (19)	0.0101 (5)

Atomic displacement parameters (Å²)

	U^{11}	U^{22}	U^{33}	U^{12}	U^{13}	U^{23}
Cu1	0.0171 (6)	0.0169 (15)	0.0184 (6)	−0.0019 (5)	0.0032 (4)	0.0025 (5)
Cu2	0.0171 (6)	0.0142 (13)	0.0185 (6)	0.0005 (8)	0.0037 (4)	0.0017 (4)
Fe	0.0115 (8)	0.0137 (17)	0.0093 (7)	0.000	0.0041 (6)	0.000
Ge	0.0080 (5)	0.0100 (8)	0.0096 (5)	−0.0009 (8)	0.0018 (3)	−0.0007 (4)
S1	0.0095 (13)	0.0093 (16)	0.0087 (11)	0.000	0.0014 (9)	0.000
S2	0.0089 (11)	0.0128 (15)	0.0120 (9)	−0.0029 (10)	0.0030 (7)	0.0009 (9)
S3	0.0081 (11)	0.0076 (14)	0.0122 (9)	0.0004 (8)	0.0033 (8)	−0.0003 (8)
S4	0.0101 (10)	0.0094 (13)	0.0107 (9)	−0.0012 (7)	0.0010 (7)	−0.0004 (10)

Geometric parameters (Å, º)

Cu1—S3^{i}	2.290 (2)	Fe—S4^{v}	2.331 (3)
Cu1—S3	2.302 (2)	Fe—S4	2.331 (3)
Cu1—S2^{ii}	2.303 (2)	Fe—S2^{iv}	2.337 (3)
Cu1—S1^{iii}	2.353 (2)	Fe—S2^{vi}	2.337 (3)
Cu2—S3	2.294 (2)	Ge—S3^{vii}	2.196 (2)
Cu2—S2	2.309 (2)	Ge—S2	2.221 (2)
Cu2—S4^{iv}	2.309 (2)	Ge—S4^{iii}	2.233 (2)
Cu2—S4	2.319 (2)	Ge—S1^{iii}	2.3107 (19)
S3^{i}—Cu1—S3	111.52 (5)	Ge^{viii}—S1—Ge^{ix}	109.23 (13)
S3^{i}—Cu1—S2^{ii}	108.81 (12)	Ge^{viii}—S1—Cu1^{viii}	112.37 (4)
S3—Cu1—S2^{ii}	107.60 (6)	Ge^{ix}—S1—Cu1^{viii}	109.92 (4)
S3^{i}—Cu1—S1^{iii}	112.79 (6)	Ge^{viii}—S1—Cu1^{ix}	109.92 (4)
S3—Cu1—S1^{iii}	106.23 (13)	Ge^{ix}—S1—Cu1^{ix}	112.37 (4)
S2^{ii}—Cu1—S1^{iii}	109.75 (6)	Cu1^{viii}—S1—Cu1^{ix}	102.96 (15)

S3—Cu2—S2	109.84 (6)	Ge—S2—Cu1^{x}	109.71 (8)
S3—Cu2—S4^{iv}	109.30 (11)	Ge—S2—Cu2	110.72 (12)
S2—Cu2—S4^{iv}	111.38 (6)	Cu1^{x}—S2—Cu2	109.87 (7)
S3—Cu2—S4	109.17 (7)	Ge—S2—Fe^{vii}	109.96 (9)
S2—Cu2—S4	107.49 (11)	Cu1^{x}—S2—Fe^{vii}	108.33 (14)
S4^{iv}—Cu2—S4	109.62 (5)	Cu2—S2—Fe^{vii}	108.21 (7)
S4^{v}—Fe—S4	109.72 (19)	Ge^{vi}—S3—Cu1^{viii}	108.48 (7)
S4^{v}—Fe—S2^{iv}	107.13 (6)	Ge^{vi}—S3—Cu2	109.52 (7)
S4—Fe—S2^{iv}	113.18 (6)	Cu1^{viii}—S3—Cu2	106.84 (11)
S4^{v}—Fe—S2^{vi}	113.18 (6)	Ge^{vi}—S3—Cu1	111.62 (11)
S4—Fe—S2^{vi}	107.13 (6)	Cu1^{viii}—S3—Cu1	108.31 (7)
S2^{iv}—Fe—S2^{vi}	106.58 (17)	Cu2—S3—Cu1	111.89 (8)
S3^{vii}—Ge—S2	112.97 (13)	Ge^{ix}—S4—Cu2^{xi}	107.94 (11)
S3^{vii}—Ge—S4^{iii}	109.74 (6)	Ge^{ix}—S4—Cu2	113.68 (8)
S2—Ge—S4^{iii}	110.97 (6)	Cu2^{xi}—S4—Cu2	109.46 (7)
S3^{vii}—Ge—S1^{iii}	108.92 (5)	Ge^{ix}—S4—Fe	112.60 (9)
S2—Ge—S1^{iii}	107.64 (6)	Cu2^{xi}—S4—Fe	105.12 (7)
S4^{iii}—Ge—S1^{iii}	106.34 (12)	Cu2—S4—Fe	107.68 (14)

Symmetry codes: (i) −*x*+3/2, *y*−1/2, −*z*+2; (ii) *x*, *y*−1, *z*; (iii) *x*−1/2, *y*−1/2, *z*; (iv) −*x*+3/2, *y*−1/2, −*z*+1; (v) −*x*+2, *y*, −*z*+1; (vi) *x*+1/2, *y*−1/2, *z*; (vii) *x*−1/2, *y*+1/2, *z*; (viii) −*x*+3/2, *y*+1/2, −*z*+2; (ix) *x*+1/2, *y*+1/2, *z*; (x) *x*, *y*+1, *z*; (xi) −*x*+3/2, *y*+1/2, −*z*+1.

Tetracopper cobalt digermanium heptasulfide (II)

Crystal data

$Cu_4CoGe_2S_7$
M_r = 682.69
Monoclinic, *C*2
a = 11.7280 (2) Å
b = 5.33987 (10) Å
c = 8.33133 (14) Å
β = 98.6680 (12)°
V = 515.80 (2) Å^3
Z = 2
F(000) = 638
D_x = 4.396 Mg m^{-3}
Mo *Kα* radiation, *λ* = 0.71073 Å
Cell parameters from 4827 reflections
θ = 4.2–32.6°
μ = 16.76 mm^{-1}
T = 296 K
Irregular, grey
0.08 × 0.07 × 0.06 mm

Data collection

Bruker SMART APEXII diffractometer
φ and *ω* Scans scans
Absorption correction: multi-scan (SADABS; Sheldrick, 2002)
T_{min} = 0.356, T_{max} = 0.435
2239 measured reflections
1177 independent reflections
1039 reflections with $I > 2\sigma(I)$
R_{int} = 0.017
θ_{max} = 27.5°, θ_{min} = 2.5°
h = −15→15
k = −6→6
l = −10→10

Refinement

Refinement on F^2
Least-squares matrix: full
$R[F^2 > 2\sigma(F^2)]$ = 0.030
$wR(F^2)$ = 0.075
S = 1.11
1177 reflections
67 parameters
1 restraint
Primary atom site location: structure-invariant direct methods
$w = 1/[\sigma^2(F_o^2) + 3.9921P]$ where $P = (F_o^2 + 2F_c^2)/3$
$(\Delta/\sigma)_{max} < 0.001$
$\Delta\rho_{max}$ = 0.88 e Å^{-3}
$\Delta\rho_{min}$ = −0.49 e Å^{-3}

Extinction correction: *SHELXL2018/3* (Sheldrick 2015), $Fc^*=kFc[1+0.001xFc^2\lambda^3/\sin(2\theta)]^{-1/4}$

Extinction coefficient: 0.060 (3)
Absolute structure: Flack (1983)
Absolute structure parameter: 0.06 (3)

Special details

Geometry. All esds (except the esd in the dihedral angle between two l.s. planes) are estimated using the full covariance matrix. The cell esds are taken into account individually in the estimation of esds in distances, angles and torsion angles; correlations between esds in cell parameters are only used when they are defined by crystal symmetry. An approximate (isotropic) treatment of cell esds is used for estimating esds involving l.s. planes.

Refinement. Refined as a two-component inversion twin

Fractional atomic coordinates and isotropic or equivalent isotropic displacement parameters (Å²)

	x	*y*	*z*	U_{iso}*/U_{eq}
Cu1	0.64303 (9)	0.2051 (4)	0.93412 (12)	0.0177 (7)
Cu2	0.71154 (9)	0.7108 (2)	0.64143 (12)	0.0158 (6)
Co	1.000000	0.7206 (7)	0.500000	0.0141 (8)
Ge	0.42703 (6)	0.7276 (4)	0.78209 (9)	0.0092 (4)
S1	1.000000	0.9762 (6)	1.000000	0.0090 (6)
S2	0.56898 (15)	0.9604 (5)	0.7167 (2)	0.0118 (6)
S3	0.78425 (15)	0.4533 (4)	0.8520 (2)	0.0092 (6)
S4	0.85742 (15)	0.9682 (5)	0.5803 (2)	0.0094 (5)

Atomic displacement parameters (Å²)

	U^{11}	U^{22}	U^{33}	U^{12}	U^{13}	U^{23}
Cu1	0.0181 (6)	0.0182 (18)	0.0167 (6)	−0.0026 (5)	0.0023 (4)	0.0018 (6)
Cu2	0.0168 (6)	0.0131 (14)	0.0175 (6)	0.0004 (8)	0.0029 (4)	0.0014 (6)
Co	0.0118 (7)	0.021 (2)	0.0096 (7)	0.000	0.0028 (5)	0.000
Ge	0.0090 (5)	0.0100 (9)	0.0086 (5)	−0.0011 (7)	0.0012 (3)	−0.0019 (6)
S1	0.0102 (12)	0.0092 (18)	0.0072 (11)	0.000	−0.0001 (9)	0.000
S2	0.0101 (9)	0.0160 (15)	0.0097 (9)	−0.0022 (11)	0.0028 (7)	−0.0007 (9)
S3	0.0095 (9)	0.0076 (16)	0.0109 (9)	0.0012 (8)	0.0025 (7)	0.0017 (9)
S4	0.0113 (9)	0.0090 (13)	0.0076 (8)	−0.0008 (7)	0.0008 (7)	−0.0012 (10)

Geometric parameters (Å, º)

Cu1—S3^{i}	2.292 (2)	Co—S4^{v}	2.308 (3)
Cu1—S2^{ii}	2.295 (2)	Co—S4	2.308 (3)
Cu1—S3	2.304 (2)	Co—S2^{iv}	2.325 (3)
Cu1—S1^{iii}	2.343 (3)	Co—S2^{vi}	2.325 (3)
Cu2—S3	2.290 (2)	Ge—S2	2.211 (3)
Cu2—S2	2.298 (3)	Ge—S3^{vii}	2.211 (2)
Cu2—S4^{iv}	2.301 (2)	Ge—S4^{iii}	2.236 (2)
Cu2—S4	2.311 (2)	Ge—S1^{iii}	2.316 (2)
S3^{i}—Cu1—S2^{ii}	109.37 (12)	Ge^{viii}—S1—Ge^{ix}	109.14 (15)
S3^{i}—Cu1—S3	111.62 (6)	Ge^{viii}—S1—Cu1^{viii}	111.56 (4)
S2^{ii}—Cu1—S3	107.25 (7)	Ge^{ix}—S1—Cu1^{viii}	110.41 (4)

S3^{i}—Cu1—S1^{iii}	112.08 (6)	Ge^{viii}—S1—Cu1^{ix}	110.41 (4)
S2^{ii}—Cu1—S1^{iii}	109.73 (7)	Ge^{ix}—S1—Cu1^{ix}	111.56 (4)
S3—Cu1—S1^{iii}	106.65 (13)	Cu1^{viii}—S1—Cu1^{ix}	103.68 (17)
S3—Cu2—S2	109.96 (7)	Ge—S2—Cu1^{x}	109.59 (8)
S3—Cu2—S4^{iv}	108.79 (11)	Ge—S2—Cu2	110.30 (13)
S2—Cu2—S4^{iv}	111.31 (7)	Cu1^{x}—S2—Cu2	109.95 (8)
S3—Cu2—S4	108.88 (8)	Ge—S2—Co^{vii}	109.91 (9)
S2—Cu2—S4	107.97 (11)	Cu1^{x}—S2—Co^{vii}	108.57 (14)
S4^{iv}—Cu2—S4	109.90 (5)	Cu2—S2—Co^{vii}	108.48 (8)
S4^{v}—Co—S4	110.11 (19)	Ge^{vi}—S3—Cu2	109.57 (8)
S4^{v}—Co—S2^{iv}	107.45 (6)	Ge^{vi}—S3—Cu1^{viii}	108.46 (8)
S4—Co—S2^{iv}	112.63 (7)	Cu2—S3—Cu1^{viii}	107.17 (11)
S4^{v}—Co—S2^{vi}	112.63 (7)	Ge^{vi}—S3—Cu1	111.81 (11)
S4—Co—S2^{vi}	107.45 (6)	Cu2—S3—Cu1	111.81 (8)
S2^{iv}—Co—S2^{vi}	106.59 (18)	Cu1^{viii}—S3—Cu1	107.84 (7)
S2—Ge—S3^{vii}	112.75 (14)	Ge^{ix}—S4—Cu2^{xi}	107.42 (11)
S2—Ge—S4^{iii}	111.49 (7)	Ge^{ix}—S4—Co	111.98 (10)
S3^{vii}—Ge—S4^{iii}	109.30 (7)	Cu2^{xi}—S4—Co	105.80 (7)
S2—Ge—S1^{iii}	108.43 (7)	Ge^{ix}—S4—Cu2	113.66 (9)
S3^{vii}—Ge—S1^{iii}	108.34 (6)	Cu2^{xi}—S4—Cu2	109.24 (7)
S4^{iii}—Ge—S1^{iii}	106.29 (12)	Co—S4—Cu2	108.42 (14)

Symmetry codes: (i) −*x*+3/2, *y*−1/2, −*z*+2; (ii) *x*, *y*−1, *z*; (iii) *x*−1/2, *y*−1/2, *z*; (iv) −*x*+3/2, *y*−1/2, −*z*+1; (v) −*x*+2, *y*, −*z*+1; (vi) *x*+1/2, *y*−1/2, *z*; (vii) *x*−1/2, *y*+1/2, *z*; (viii) −*x*+3/2, *y*+1/2, −*z*+2; (ix) *x*+1/2, *y*+1/2, *z*; (x) *x*, *y*+1, *z*; (xi) −*x*+3/2, *y*+1/2, −*z*+1.